Electronic Supplementary Information

Experimental section

Materials: Cobalt nitrate hexahydrate ($Co(NO_3)_2·6H_2O$, 99.9%), 2-methylimidazole (99%), glucose (99.99%), potassium chloroplatinate (K_2PtCl_6, 99%), ascorbic acid (AA, >99.99%), sodium chloride (NaCl, >99.5%), sucrose (99.9%), fructose (99%), uric acid (UA, >99.99%), dopamine (DA, >99%), and potassium chloride (KCl, 99%) were purchased from Shanghai Titan Scientific Co., Ltd. Nitric acid (HNO_3) and ethanol (99%) were obtained from Beijing Chemical Reagent Co., Ltd. All reagents were of analytical grade and used as received without further purification. Carbon cloth (CC, 0.3 mm thick) was supplied by Suzhou Sinero Technology Co., Ltd. The human serum was provided by West China Hospital, Sichuan University. The SH-SY5Y human neuroblastoma cell-specific culture medium was purchased from Sichuan Weiao xincheng Biotechnology Co., Ltd.

Materials synthesis:

Synthesis of ZIF-67/CC: The bare CC was first cleaned by sequential ultrasonication in ethanol and deionized water, followed by nitric acid treatment to improve surface wettability. After rinsing and drying, a clean CC substrate was obtained. Subsequently, the cobalt-based metal–organic framework, namely zeolitic imidazolate frameworks-67 (ZIF-67), was grown in situ on the CC substrate in a nanosheet-like form. 1.31 g of 2-methylimidazole and 0.582 g of $Co(NO_3)_2·6H_2O$, used as the precursors for ZIF-67, were separately dissolved in 40 mL of deionized water and stirred for 3 min, followed by rapid mixing to form a purple solution. The resulting solution was then poured into a Petri dish containing the pretreated CC. After standing for 2 h, nanosheet-like ZIF-67 grew in situ on the carbon fibers of CC, forming the ZIF-67 nanoarray on CC (ZIF-67/CC).

Synthesis of CoO@NC/CC: The obtained ZIF-67/CC was then thermally treated under an argon atmosphere. The temperature was increased to 350°C at a heating rate of 2°C min^{-1} and maintained for 1 h, followed by further heating to 500°C at 3°C min^{-1} and holding for 2 h. After cooling to room temperature, the organic ligands

were carbonized to form N-doped carbon, and the cobalt species were transformed into CoO. The derived CoO@NC nanoarray remained directly attached to the CC after pyrolysis, thereby forming a self-supported CoO@NC/CC electrode.

Synthesis of Pt/CoO@NC/CC: Pt nanoparticles were loaded onto CoO@NC/CC through a spontaneous redox reaction. Briefly, 0.5 mg of K_2PtCl_6 was dissolved in 10 mL of deionized water. The CoO@NC/CC electrode was immersed in the solution for 60 min at room temperature. The electrode was then removed, rinsed with deionized water, and dried at 60 °C to obtain the final Pt/CoO@NC/CC electrode.

Characterizations: X-ray diffraction (XRD) measurements were carried out using an XRDynamic 500 diffractometer (Anton Paar, Austria). X-ray photoelectron spectroscopy (XPS) analyses were performed on a Thermo Scientific K-Alpha system. Scanning electron microscopy (SEM) images were obtained using a Thermo Scientific Apreo 2C microscope, while transmission electron microscopy (TEM) observations were conducted on a Talos F200S electron microscope.

Electrochemical measurements: The electrochemical performance of Pt/CoO@NC/CC and CoO@NC/CC electrodes (0.25 × 0.25 cm^2) was evaluated using a conventional three-electrode configuration on a DH7003D electrochemical workstation. A platinum wire and an Hg/HgO electrode were employed as the counter and reference electrodes, respectively, while the prepared Pt/CoO@NC/CC electrode served as the working electrode. Cyclic voltammetry (CV) measurements were carried out over a potential range from −0.4 to 0.9 V. Chronoamperometric (CA) glucose sensing was conducted at an applied potential of 0.62 V using 0.1 M KOH as the electrolyte for both CV and CA measurements. All potentials are reported versus the Hg/HgO reference electrode without correction.

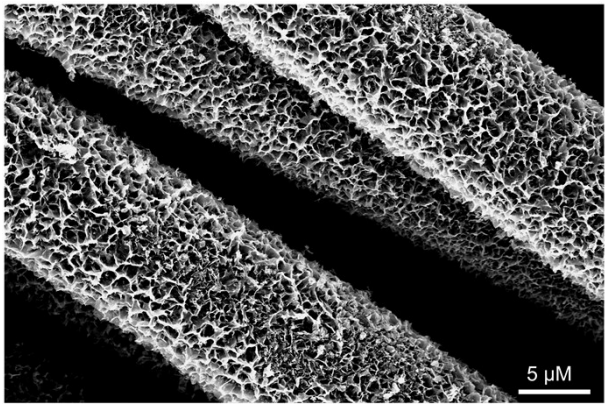

Fig. S1. SEM image of CoO@NC/CC.

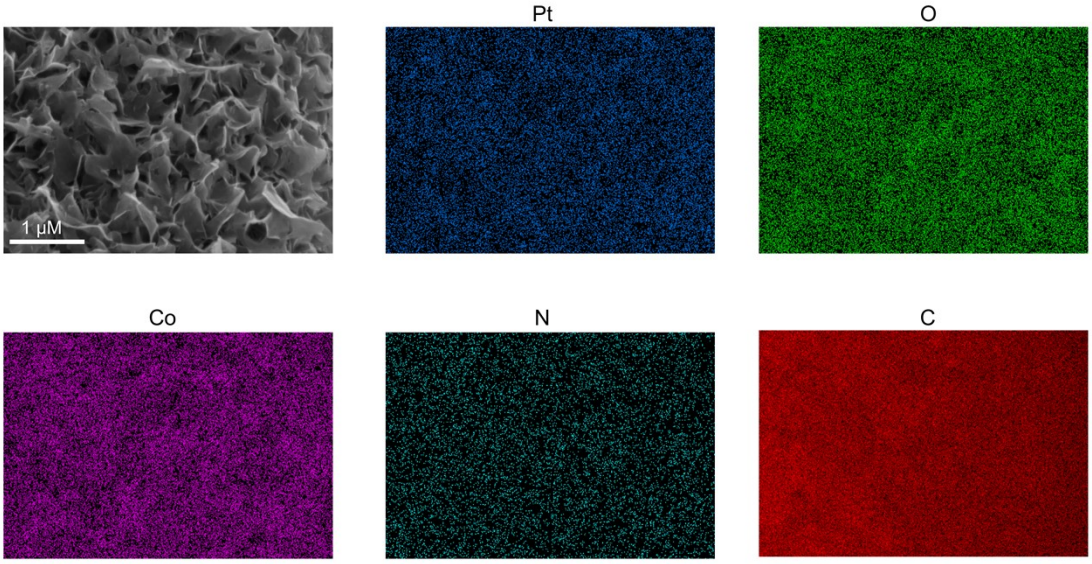

Fig. S2. SEM and its corresponding EDX elemental mapping images of Pt/CoO@NC/CC.

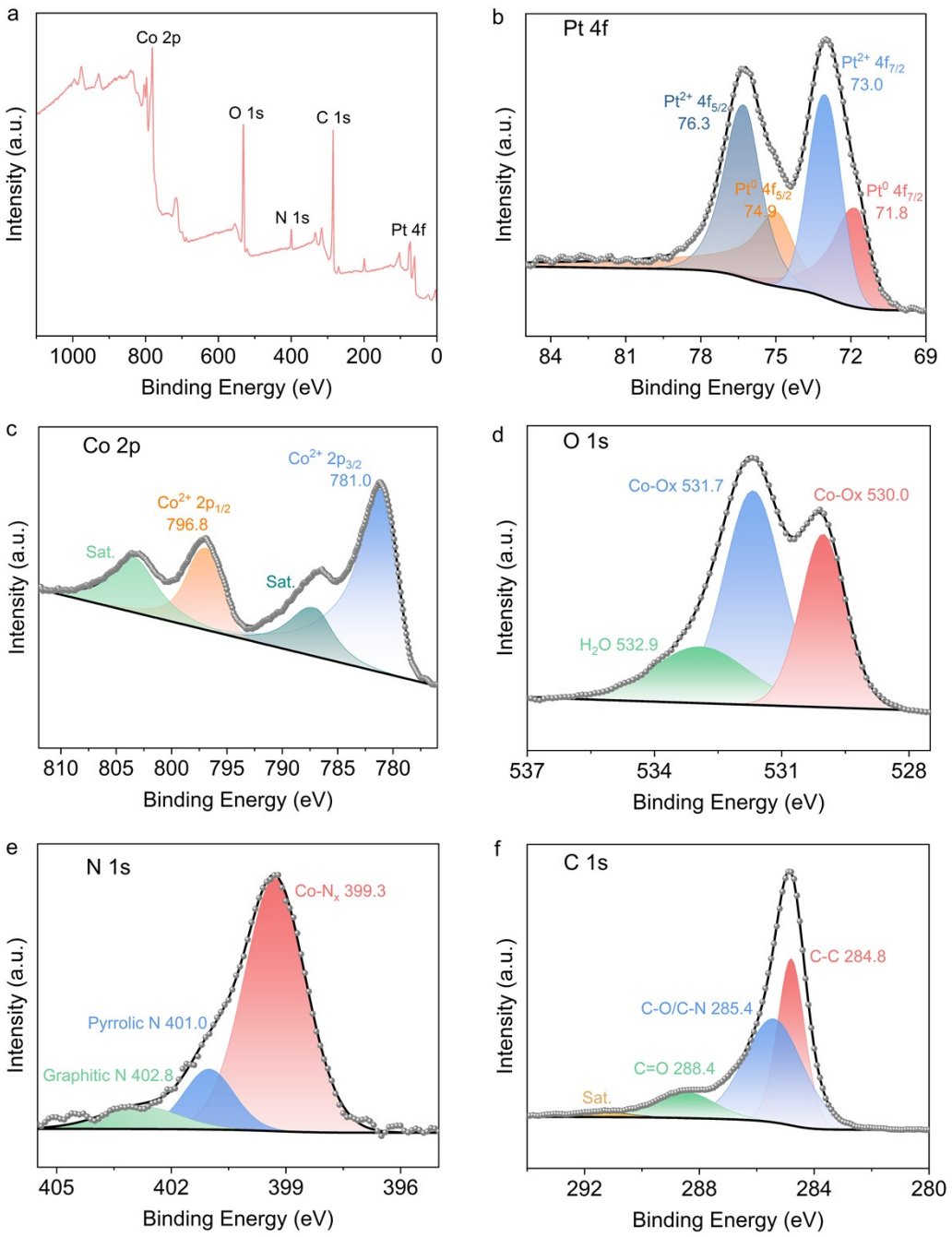

Fig.S3. (a) XPS survey spectrum of Pt/CoO@NC/CC. (b–f) High-resolution XPS spectra of Pt/CoO@NC/CC in the Pt 4*f*, Co 2*p*, O 1*s*, N 1*s*, and C 1*s* regions, respectively.

XPS analysis further confirms the successful incorporation of Pt into CoO@NC/CC. The survey spectrum (Fig. S3a) reveals the presence of Pt, Co, O, N, and C. In the Pt 4*f* region (Fig. S3b), peaks at 71.8 and 74.9 eV correspond to metallic Pt^0 $4f_7/_2$ and $4f_5/_2$, respectively, consistent with HRTEM observations[1-3], while additional peaks at 73.0 and 76.3 eV are assigned to Pt^{2+} species arising from surface oxidation[4,5]. The

Co 2*p* spectrum (Fig. S3c) displays dominant Co^{2+} features and satellite peaks[6-9]. The O 1*s* spectrum (Fig. S3d) indicates Co-O_x bonds and adsorbed H_2O[10]. Furthermore, the N 1*s* and C 1*s* spectra (Fig. S3e,f) confirm the presence of Co–N species, nitrogen-doped carbon, and diverse carbon bonding configurations[3,11,12].

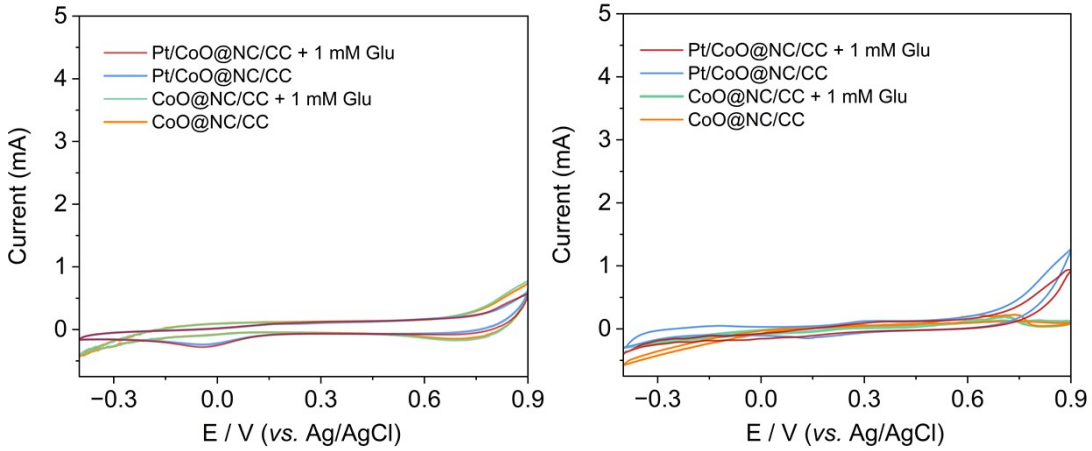

Fig. S4. CV curves of Pt/CoO@NC/CC and CoO@NC/CC electrodes recorded in 0.1 M PB buffer with and without glucose (left: pH 7.4; right: pH 3.0).

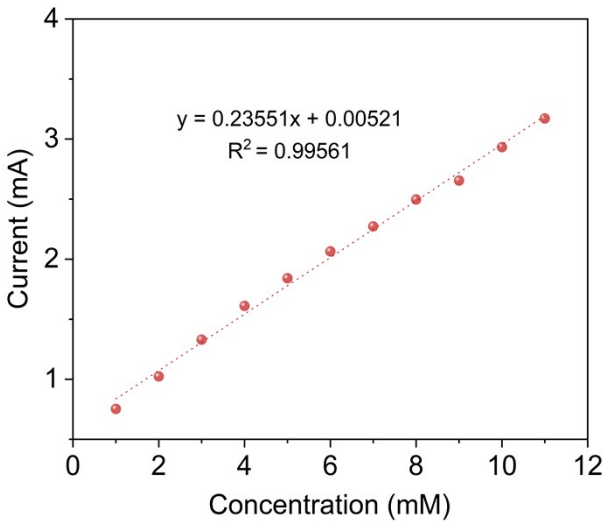

Fig. S5. Correlation between the oxidation peak current of the Pt/CoO@NC/CC electrode and glucose concentration.

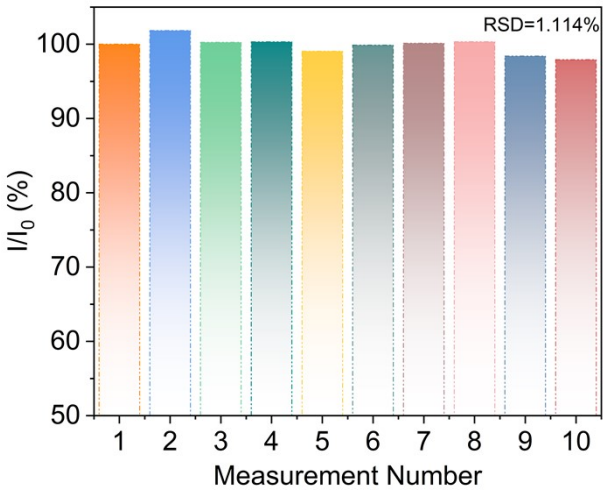

Fig. S6. Repeated tests on the Pt/CoO@NC/CC electrode.

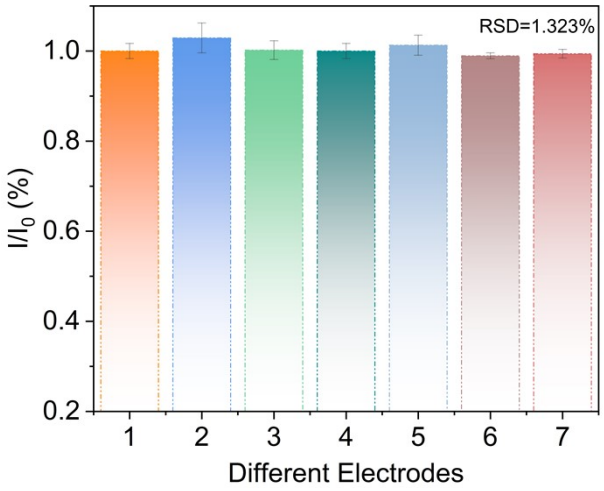

Fig. S7. Reproducibility tests of inter-electrode.

Table S1. Comparison of the glucose sensing performance of Pt/CoO@NC/CC with other reported Pt-based electrodes.

Electrodes	Sensitivity ($\mu A\ mM^{-1}\ cm^{-2}$)	Linear range (mM)	LOD (μM)	Ref.
Pt/CoO@NC/CC	**2866 and 518**	**0.001-4**	**0.4**	**This work**
Pt_1-NiCo-LDH/$Ti_3C_2T_x$	506.6	0.04-0.55	0.035	13
Pd@Pt CNCC	11.06	2.4-10.6	0.15	14
GO/MWCNT/Au@Pt/GCE	330	0.00005-2.5	0.042	15
PtNF-rGO/GCE	335.5	0.3-3.5	53	16
Pt_1/$Ni(OH)_2$/NG	220.75	0.01-2.18	/	17
$PtNi_{(1:3)}$ hydrogel/GCE	19.75	0-2.5	67	18
Pt-NPs/MnPc-Mn/Au	25.48	0-0.8	5.5	19
Pt_1/Cu@CuO NWs	852.163	0.00001-0.00518	3.6	20
Pt/MXene	3.43	0-8	29.15	21
$Pt_{75}Cu_{25}NC$	135	0.01-17	2.5	22

Table S2. Recovery tests of the Pt/CoO@NC/CC electrode in human serum and cell culture medium.

Sample	Added glucose (mM)	Found (mM)	Recovery (%)	RSD (%) (n=3)
Human blood serum	0.2	0.1996	99.82	1.275
	0.4	0.4072	101.79	3.450
	0.6	0.5977	99.61	2.597
Cell culture medium	0.2	0.2007	100.36	4.431
	0.4	0.4121	103.02	1.772
	0.6	0.6145	102.41	3.781

References

1 Z. Li, J. Zou, X. Xi, P. Fan, Y. Zhang, Y. Peng, D. Banham, D. Yang and A. Dong, *Adv. Mater.*, 2022, **34**, e2202743.

2 M. Guo, Q. Meng, M.-L. Gao, L. Zheng, Q. Li, L. Jiao and H.-L. Jiang, *Angew. Chem. Int. Ed.*, 2025, **64**, e202418964.

3 L. Huang, M. Wei, R. Qi, C.-L. Dong, D. Dang, C.-C. Yang, C. Xia, C. Chen, S. Zaman, F.-M. Li, B. You and B.-Y. Xia, *Nat. Commun.*, 2022, **13**, 6703.

4 D. Fantauzzi, S. Krick Calderón, J. E. Mueller, M. Grabau, C. Papp, H.-P. Steinrück, T. P. Senftle, A. C. van Duin and T. Jacob, *Angew. Chem. Int. Ed.*, 2017, **56**, 2594–2598.

5 R. Mom, L. Frevel, J.-J. Velasco-Vélez, M. Plodinec, A. Knop-Gericke and R. Schlögl, *J. Am. Chem. Soc.*, 2019, **141**, 6537-6544.

6 L. Bai, X. Wen and J. Guan, *ACS Appl. Energy Mater.*, 2019, **2**, 5584–5590.

7 L. Qin, J.-L. Liu, X.-Y. Zhou, Y.-Q. Wang, X. Sun and M.-D. Zhang, *Energy Fuels*, 2022, **36**, 5843–5851.

8 Y. Li, Z. Jin and T. Zhao, *Chem. Eng. J.*, 2020, **382**, 123051.

9 A. Indra, P. W. Menezes, I. Zaharieva, H. Dau and M. Driess, *J. Mater. Chem. A*, 2020, **8**, 2637–2643.

10 Q. Xu, R. Qiu, H. Jiang and X. Wang, *J. Electroanal. Chem.*, 2019, **839**, 247–255.

11 Z. Chen, R. Wu, Y. Liu, Y. Ha, Y. Guo, D. Sun, M. Liu and F. Fang, *Adv. Mater.*, 2018, **30**, e1802011.

12 F. Risplendi, N. Garino, J. Zeng, A. Sacco, S. Mehta, C. Deriu, L. Fabris, M. Fontana, A. Chiodoni, G. Cicero and M. Castellino, *npj 2D Mater. Appl.*, 2025, **9**, 83.

13 Y. Zhang, Q. Huang, Z.-H. Sun, R. Zheng, Y. Ma, D. Han and L. Niu, *Anal. Chem.*, 2024, **96**, 18239-18245.

14 S.-S. Wang, W.-J. Qiu, T.-P. Wang and C.-L. Lee, *Appl. Surf. Sci.*, 2022, **605**, 154670.

15 R. Wang, X. Liu, Y. Zhao, J. Qin, H. Xu, L. Dong, S. Gao and L. Zhong, *Microchem. J.*, 2022, **174**, 107061.

16 S. Gengan, R. M. Gnanamuthu, S. Sankaranarayanan, V. M. Reddy, B. C. Marepally and R. K. Biroju, *Sensor. Actuat. A-Phys.*, 2023, **353**, 114232.

17 B. Long, Y. Zhao, P. Cao, W. Wei, Y. Mo, J. Liu, C.-J. Sun, X. Guo, C. Shan and M.-H. Zeng, *Anal. Chem.*, 2022, **94**, 1919-1924.

18 G. Li, C. Wang, Y. Chen, F. Liu, H. Fan, B. Yao, J. Hao, Y. Yu and D. Wen, *Small*, 2023, **19**, e2206868.

19 W. Huang, Y. Yang, Y. Xu, F. Xiao and L. Wang, *Adv. Sci.*, 2025, **12**, e07212.

20 Y. Zhao, Y. Jiang, Y. Mo, Y. Zhai, J. Liu, A. C. Strzelecki, X. Guo and C. Shan, *Small*, 2023, **19**, e2207240.

21 Q.-F. Li, X. Chen, H. Wang, M. Liu and H.-L. Peng, *ACS Appl. Mater. Interfaces*, 2023, **15**, 13290-13298.

22 X. Cao, N. Wang, S. Jia and Y. Shao, *Anal. Chem.*, 2013, **85**, 5040-5046.